DOI: 10.64302/joshusc.v31n1c.1315

PHOTOLUMINESCENCE OF PHYTOCAPPED CARBON QUANTUM DOTS MODIFIED WITH GOLD NANOPARTICLES

Le Anh Thi[1,2], Vo Thanh Tung[3] , Lam Thi Bich Tran[4], Do Hoang Tung[5], Nguyen Nhu Le[6], Le Thi Kim Dung[7], Tran Duy Quynh Nhu[7], Nguyen Minh Hoa[7]*

[1] Institute of Research and Development, Duy Tan University, Danang, Vietnam

[2] Faculty of Natural Sciences, Duy Tan University, Danang, Vietnam

[3] University of Sciences, Hue University, Hue, Vietnam

[4] Ho Chi Minh City University of Education, Gialai, Vietnam

[5] Institute of Physics, Vietnam Academy of Science and Technology, Hanoi, Vietnam

[6] Faculty of Physics, University of Education, Hue University, Viet Nam

[7] Faculty of Fundamental Sciences, Hue University of Medicine and Pharmacy, Hue University, Hue, Vietnam

*Email: nguyenminhoa@hueuni.edu.vn; nmhoa@huemed-univ.edu.vn

Received: 8/9/2025; Received in revised form: 02/10/2025; Accepted: 13/10/2025

ABSTRACT

This study investigates the synthesis and characterization of carbon quantum dots (CQDs) derived from orange juice through a plasma-solution interaction method, followed by functionalization with gold nanoparticles (AuNPs). The CQDs exhibited strong blue photoluminescence upon excitation at 390 nm, with a photoluminescence quantum yield (PLQY) of 21.9%. The CQDs were spherical, with an average size of 3.5 nm, while the AuNPs had an average size of 18 nm. The resulting Au@CQDs nanohybrids (NHs) demonstrated an increase in size to more than 20.2 nm. UV-vis absorption and photoluminescence spectroscopy confirmed the interaction between CQDs and AuNPs, with the nanohybrids displaying plasmon-enhanced fluorescence. This study presents an eco-friendly approach for the synthesis of CQDs and their hybridization with AuNPs, emphasizing the effect of surface modification on their photoluminescent properties, with potential applications in sensing and photonic devices.

Keywords: Carbon quantum dots, photoluminescence, phytocapped, AuNPs, surface modification.

1. INTRODUCTION

Carbon quantum dots (CQDs) are an emerging class of zero-dimensional nanomaterials that have attracted significant attention owing to their unique optical, chemical, and structural properties [1,2]. Typically smaller than 10 nm, CQDs exhibit strong and tunable photoluminescence (PL), high water solubility, chemical stability, and excellent biocompatibility, making them promising for a wide range of applications including optoelectronics, sensing, catalysis, and bioimaging [3–6]. Recently, sustainable and green synthesis strategies for CQDs have gained interest as alternatives to conventional chemical oxidation or high-temperature processes. Natural precursors such as fruit extracts, plant leaves, and other biomass sources are abundant in carbon-rich compounds and functional groups, enabling environmentally friendly synthesis of highly emissive CQDs [7,8]. In particular, orange juice is rich in citric acid and sugars, which promote efficient carbonization and surface passivation, leading to CQDs with strong fluorescence and high quantum yield [9,10].

Surface modification and hybridization have been widely applied to further improve the optical performance of CQDs. Among them, the combination of CQDs with noble metal nanoparticles such as gold nanoparticles (AuNPs) has attracted special interest due to the localized surface plasmon resonance (LSPR) effect of AuNPs [11]. This plasmonic interaction can enhance CQD fluorescence, modulate emission spectra, and improve photostability, giving rise to hybrid nanostructures (CQDs@AuNPs) with advanced optical responses [12]. Such nanohybrids integrate the photoluminescent and biocompatible nature of CQDs with the unique plasmonic features of AuNPs, making them suitable for applications in sensing, imaging, and photonic devices. Despite extensive work on hydrothermal and microwave-assisted methods for CQD synthesis, the plasma solution interaction technique remains relatively underexplored. Plasma-based synthesis offers several advantages, including rapid reaction times, mild conditions, and the absence of toxic reagents [9,13]. Moreover, plasma-induced chemistry facilitates the incorporation of abundant oxygen-containing functional groups, improving luminescence efficiency and stability.

In this work, we report the synthesis of phytocapped carbon quantum dots (CQDs) derived from orange juice using a plasma solution interaction method, followed by modification with gold nanoparticles (AuNPs) to form Au@CQDs nanohybrids (NHs). The optical properties of the nanomaterials were systematically characterized using UV–vis absorption and photoluminescence spectroscopy. The as-prepared CQDs exhibited strong blue emission at 390 nm, with a relative quantum yield of 21.9%. Morphological analysis using TEM, SEM, and HR-TEM revealed spherical structures with average sizes of 3.5 nm for CQDs, 18.2 nm for AuNPs, and over 20 nm for the NHs. These findings provide new insights into the role of green precursors and surface

modification in tuning the luminescent properties of CQDs, highlighting the potential of plasma-assisted synthesis for producing advanced fluorescent nanomaterials.

2. EXPERIMENTAL SECTION

2.1. Materials

Fresh orange juice was employed as the carbon precursor for CQD synthesis. Chloroauric acid ($HAuCl_4 \cdot 3H_2O$, analytical grade) was used as the gold source for nanoparticle preparation. All reagents were of analytical grade and used without further purification. Deionized water (18.2 MΩ·cm) was used throughout the experiments.

The overall experimental procedure is illustrated in **Figure 1**. Details for the synthesis of CQDs from orange juice, AuNPs from orange peels, and the final Au@CQDs nanohybrids are provided in the following sections.

2.2. Synthesis of Carbon Quantum Dots (CQDs)

CQDs were synthesized using a plasma solution interaction method. Freshly squeezed orange juice was filtered to remove pulp and directly used as the carbon precursor without dilution. The filtered orange juice (50 mL) was transferred into a quartz reactor. Plasma discharge was generated using a high-voltage AC power supply (5 kV), with stainless steel electrodes immersed in the solution at a fixed gap of 5 mm. Plasma treatment was carried out for 15 minutes under continuous stirring. During the exposure, energetic electrons and reactive species induced the carbonization of organic molecules in the orange juice, resulting in the formation of fluorescent CQDs [9]. The resulting brownish-yellow solution was centrifuged at 10,000 rpm for 15 minutes and filtered through a 0.22 μm syringe filter to remove larger particulates. The purified CQD solution was then stored at 4 °C for further use.

Figure 1. Schematic illustration of the synthesis process for CQDs from orange juice, AuNPs from orange peels, and the subsequent formation of Au@CQDs NHs.

2.3. Synthesis of Gold Nanoparticles (AuNPs)

AuNPs were synthesized via a plasma-assisted reduction method. An aqueous solution of $HAuCl_4$ (1 mM, 50 mL) was directly mixed with freshly orange peels, which served as the reducing and capping agent. The mixture was subjected to plasma treatment using a high-voltage AC power supply (5 kV) for 15 minutes, under continuous stirring. The plasma-induced energetic electrons and reactive species facilitated the reduction of Au^{3+} ions, leading to the formation of gold nanoparticles [14,15]. The color of the solution changed from pale yellow to ruby red, confirming AuNP formation. The nanoparticles were collected by centrifugation at 10,000 rpm for 10 minutes, washed twice with deionized water, and redispersed in water.

2.4. Preparation of Au@CQDs NHs

The Au@CQDs NHs were prepared by mixing the synthesized CQDs with AuNPs under plasma treatment. Typically, 20 mL of CQD solution was mixed with 20 mL of AuNP solution (1 mg/mL). The pH of the mixture was adjusted to approximately 9 using 0.1 M NaOH to promote surface interaction. The mixture was then subjected to plasma treatment at 5 kV for 15 minutes under continuous stirring. The plasma treatment facilitated electrostatic interactions and the binding of AuNPs to the surface functional groups (–COOH, –OH) of the CQDs, forming the Au@CQDs NHs [12,16]. The resulting nanohybrids were purified by centrifugation and stored at 4 °C for further use.

2.5. Characterization Techniques

UV-vis absorption spectroscopy (Varian Cary 5000, 200–800 nm) was used to study electronic transitions in the samples. Photoluminescence (PL) spectroscopy was performed using the FLS1000 Photoluminescence Spectrometer (Edinburgh Instruments) to measure the emission spectra and Photoluminescence quantum yield (PLQY). Before recording the PL spectra, all samples (CQDs and Au@CQDs NHs) were diluted to ensure that the optical density (OD) at the excitation wavelength (320–500 nm) was below 0.1 (in a 1 cm quartz cuvette) in order to minimize inner-filter effects and obtain reliable PL intensity. High-resolution transmission electron microscopy (HR-TEM) and transmission electron microscopy (TEM) (JEOL JEM-1010, 80 kV) were employed to analyze the morphology and particle size distribution. Fourier-transform infrared spectroscopy (FTIR, Jasco FT/IR-6700) was used to identify surface functional groups and structural features. Scanning electron microscopy (SEM) images were obtained using a Hitachi SU-8010 SEM. The PLQY of the samples was determined based on the ratio between the integrated photoluminescence intensity of the sample and the scattering intensity of the reference solvent (deionized water) [17], according to the following relationship:

$$PLQY(\%) = \frac{E_S - E_R}{S_R - S_S} \times 100$$

where E_s and S_s are the photoluminescence and scattering intensities of the sample, and E_r and S_r are the photoluminescence and scattering intensities of the reference solvent. This method allows the determination of the absolute photoluminescence efficiency of the nanomaterials relative to a blank solvent.

3. RESULTS AND DISCUSSION

3.1 Morphological of CQDs and AuNPs

The morphological characteristics of the synthesized CQDs and Au@CQDs NHs were analyzed using TEM, SEM, and HR-TEM as shown in Figure 2. The TEM image of the pristine CQDs (Fig. 2(a)) shows well-dispersed, spherical nanoparticles with an average size of approximately 3.5 nm, as confirmed by the particle size distribution in the inset histogram. This narrow size distribution indicates that the CQDs were synthesized with excellent size control, which is essential for their uniform optical properties. In contrast, the SEM image of the AuNPs (Fig. 2(b)) reveals a broader particle size distribution, with nanoparticles ranging from 14 to 22 nm, as shown by the size histogram. The AuNPs appear to form aggregates, but the distribution remains relatively uniform, typical of colloidal gold nanoparticles.

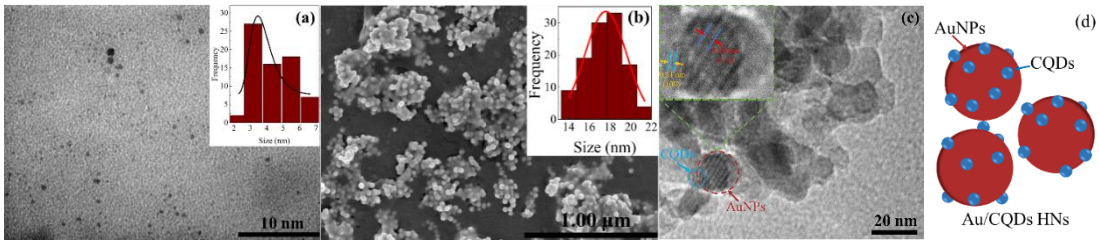

Figure 2. (a) TEM image of CQDs, (b) SEM image of AuNPs, (c) Labeled HR-TEM image of Au@CQDs NHs showing the AuNP core and CQD layer, and (d) Schematic illustration of the ideal Au@CQDs MHs structure.

The HR-TEM image of the Au@CQDs NHs (Fig. 2(c)) clearly shows the decoration of the CQDs with AuNPs. The interface between the CQDs and AuNPs is well-defined, indicating strong interactions between the two components. The lattice fringes observed in the HR-TEM image confirm the crystalline structure of the AuNPs, while the CQDs show an amorphous nature. These results demonstrate that the CQDs and AuNPs are successfully hybridized, with AuNPs decorating the surface of the CQDs, enhancing their structural stability and optical properties. A magnified view of this interface reveals distinct lattice fringes. In the core nanoparticle, a lattice spacing of 0.24 nm is measured, which corresponds to the (111) crystallographic plane of face-centered

cubic gold. This provides definitive evidence for the crystalline structure of the AuNPs. Interestingly, smaller crystalline domains are also observed within the surrounding carbonaceous layer, exhibiting a lattice spacing of 0.21 nm. This value is attributed to the (100) plane of graphitic carbon, indicating that the CQDs possess a semi-crystalline nature despite being largely amorphous. These combined observations confirm the successful formation of a tightly-bound hybrid structure composed of crystalline AuNPs decorated with semi-crystalline CQDs, enhancing their structural stability and influencing their optical properties.

3.2. FTIR Spectroscopy Analysis

The FT-IR spectra of CQDs and Au@CQDs NHs are shown in **Figure 3**. Both spectra exhibit characteristic absorption bands corresponding to oxygen-containing and hydrocarbon functional groups, which are essential for the surface passivation and stability of the nanostructures. For the CQDs, a broad absorption band centered at 3294 cm^{-1} is attributed to the stretching vibration of hydroxyl (–OH) and/or amine (–NH) groups, indicating the presence of abundant surface passivation groups derived from the organic molecules in orange juice [9]. Peaks at 2992 and 2909 cm^{-1} correspond to C–H stretching vibrations from aliphatic groups, confirming partial carbonization of sugars and citric acid precursors. A strong band at 1640 cm^{-1} is associated with C=O stretching vibrations of carbonyl and carboxyl groups, while the absorptions at 1452–1225 cm^{-1} are due to C–O and C–N stretching, typical of alcohols, esters, and amines. The band at 1050 cm^{-1} is assigned to C–O–C stretching vibrations, confirming the presence of ether linkages [18]. These features collectively demonstrate that the CQDs are decorated with abundant oxygen- and nitrogen-containing groups, which enhance dispersibility and luminescence.

In the case of Au@CQDs NHs, all major functional groups observed in the pristine CQDs are retained, but noticeable intensity changes and slight shifts are evident. The –OH/–NH stretching band (3294 cm^{-1}) and C–H stretching bands (2992–2909 cm^{-1}) show reduced intensity, suggesting partial interaction of the surface hydroxyl and carboxyl groups with AuNPs. The carbonyl band at 1640 cm^{-1} becomes more prominent in the nanohybrid, likely due to coordination interactions between Au atoms and the –COOH groups of CQDs. Additionally, the region between 1452–1225 cm^{-1} shows peak broadening in Au@CQDs NHs, consistent with enhanced interactions between AuNPs and carboxylate and hydroxyl functional groups [19].

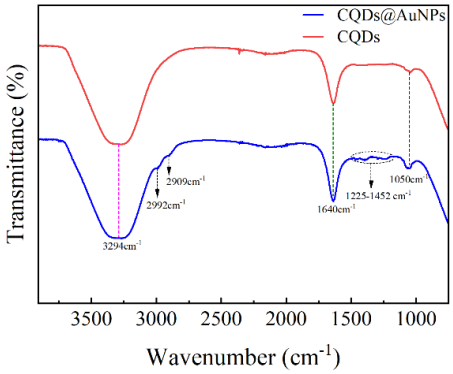

Figure 3. FTIR spectrum of CQDs and Au@CQDs nanohybrids.

These spectral differences provide strong evidence for the successful anchoring of AuNPs onto CQDs through electrostatic and coordination interactions with surface functional groups such as –OH, –COOH, and –C=O. The retention of abundant oxygenated groups ensures good aqueous dispersibility of the nanohybrids. It is important to clarify why a dedicated hybridization step is necessary and why the Au@CQDs nanohybrids do not form directly during the AuNP synthesis. The primary reason lies in the surface chemistry dictated by pH. The stable binding of AuNPs to the CQD surface relies on the electrostatic attraction with the negatively charged carboxylate groups ($–COO^-$) on the CQDs [20,21]. This is achieved by adjusting the pH to a basic condition (~9) during our hybridization step. In contrast, the one-pot synthesis of AuNPs occurs in a highly acidic environment, where the CQD surface groups would remain protonated (–COOH), thus lacking the negative charge required for stable hybrid formation. Furthermore, the rapid reduction of Au^{3+} ions is the dominant reaction pathway, consuming the reducing agents before significant carbonization into stable CQDs can occur.

3.3. Opticals properties

3.3.1. UV–Vis Absorption Spectroscopy

As shown in Figure 4, the UV-Vis absorption spectrum of the pristine CQDs displayed strong absorption bands at 223 and 282 nm, corresponding to the π–π* transition of aromatic C=C bonds and the n–π* transition of C=O groups, respectively [4]. These features are typical of carbon quantum dots, indicating the presence of conjugated domains and oxygen-containing surface functionalities. In contrast, the AuNPs exhibited a distinct absorption peak at ~540 nm, characteristic of the surface plasmon resonance (SPR) of metallic gold nanoparticles.

Interestingly, the spectrum of the Au@CQDs NHs nanohybrid displayed the characteristic absorption peaks of CQDs at 225 and 285 nm, but the SPR peak of AuNPs at ~540 nm was completely quenched. This quenching of the plasmon resonance suggests a strong electronic interaction at the interface between the CQD surface

functional groups (–OH, –COOH) and the Au atoms. Instead of coexisting as separate entities, the strong coupling likely alters the dielectric environment around the AuNPs and introduces efficient energy transfer pathways, leading to the suppression of the collective electron oscillations [19,22]. This observation confirms the successful formation of a tightly-bound hybrid structure and indicates a significant modification of the nanomaterials' optical properties.

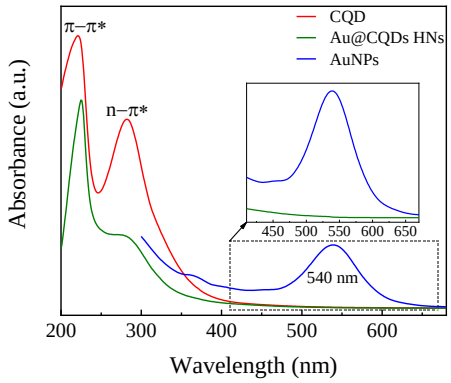

Figure 4. UV-vis absorption spectra of CQDs, AuNPs, and Au@CQDs NHs, with an inset showing a zoomed-in view of the plasmon resonance region.

3.3.2. Photoluminescence (PL) Properties

The excitation-dependent PL spectra of the CQDs are presented in Figure 5(a). Under excitation wavelengths ranging from 340 to 480 nm, the CQDs exhibited strong blue emission with a maximum intensity of approximately 3.5 × 10^5 a.u. at 420 nm excitation. The emission peaks progressively red-shifted from ~450 nm to ~560 nm as the excitation wavelength increased, a well-known characteristic of carbon quantum dots. This behavior is attributed to multiple emissive sites, including core-state and surface-state transitions, which contribute to the excitation-dependent luminescence. The highest emission intensity observed near 450–470 nm corresponds to a relative quantum yield of 21.9%, confirming the efficient radiative recombination of the CQDs [23].

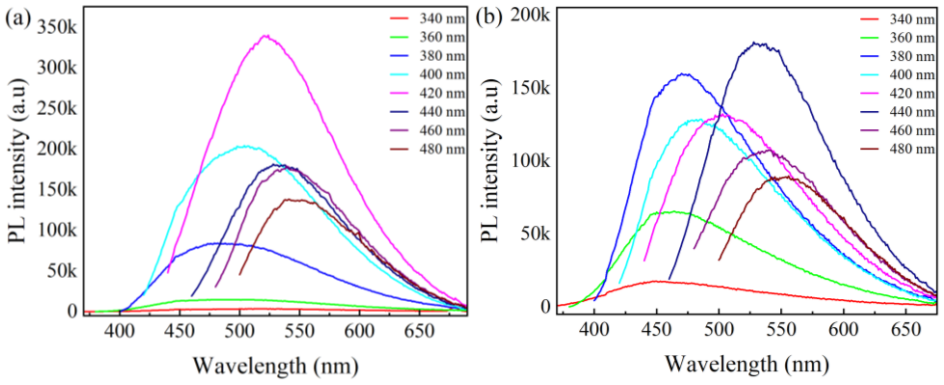

Figure 5. PL spectra of CQDs (a) and Au@CQDs NHs (b) at excitation wavelengths of 340 to 480 nm.

In contrast, the Au@CQDs NHs nanohybrid spectra in Figure 5(b) showed excitation-dependent emission between 340 and 480 nm, with the maximum PL intensity reaching approximately 1.8×10^5 a.u. at 440 nm excitation. While the overall intensity was lower than pristine CQDs, the nanohybrid exhibited noticeable spectral broadening and red-shifting. This behavior suggests that the localized surface plasmon resonance (LSPR) of AuNPs influences the recombination pathways, enhancing radiative transitions but also introducing non-radiative quenching channels [22].

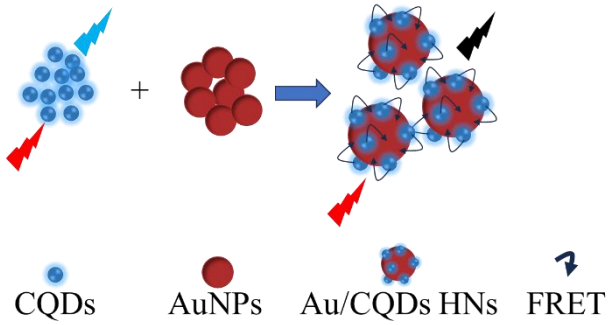

Figure 6. Schematic of the proposed photoluminescence quenching mechanism in Au@CQDs nanohybrids via non-radiative energy transfer.

The significant decrease in photoluminescence intensity, combined with the complete quenching of the surface plasmon resonance peak observed in the UV-Vis spectrum, points towards a dominant non-radiative energy transfer mechanism rather than a balance between enhancement and quenching.

These results indicate that a strong electronic coupling exists at the interface between the CQDs and AuNPs. This coupling facilitates an efficient energy transfer pathway (FRET or charge transfer), where the energy absorbed by the CQDs is transferred to the AuNPs instead of being emitted as light [19,22]. This process, illustrated in Figure 6, is responsible for the pronounced quenching of the photoluminescence and serves as strong evidence of a successful and intimate surface hybridization between the two components.

4. CONCLUSION

This study successfully synthesized carbon quantum dots (CQDs) from orange juice using a plasma-solution interaction method, followed by modification with gold nanoparticles (AuNPs) to form Au@CQDs nanohybrids. The CQDs exhibited strong blue photoluminescence with a quantum yield of 21.9%, while the nanohybrids displayed altered optical properties due to plasmonic effects. Characterization of the nanohybrids revealed a strong electronic interaction between the components, resulting in a complete quenching of the AuNPs' surface plasmon resonance and a significant quenching of the

CQDs' photoluminescence. This work highlights the critical role of surface hybridization in tuning the optical properties of CQDs and demonstrates a green, plasma-assisted method for developing advanced nanomaterials with potential applications in sensing and optoelectronics, where energy or charge transfer processes are desirable.

ACKNOWLEDGMENTS

This work is supported by the Vietnam Ministry of Education and Training (MOET) under Grant No. B2024-DHH-16.

REFERENCE

[1]. Z. Yang, T. Xu, H. Li, M. She, J. Chen, Z. Wang, S. Zhang, J. Li, (2023). Zero-Dimensional Carbon Nanomaterials for Fluorescent Sensing and Imaging. *Chemical Reviews*. **123**(18), 11047–11136.

[2]. S. Yadav, S. Daniel, (2024). Green synthesis of zero-dimensional carbon nanostructures in energy storage applications—A review. *Energy Storage*. **6**(1).

[3]. N. M. Hoa, L. D. Toan, N. Tran, L. X. Hung, L. A. Thi, (2025). Microplasma-synthesized Citrus-derived carbon quantum dots: antibacterial properties and nanoprobe sensitivity. *RSC Advances*. **15**(31), 25362–25371.

[4]. R. Lamba, Y. Yukta, J. Mondal, R. Kumar, B. Pani, B. Singh, (2024). Carbon Dots: Synthesis, Characterizations, and Recent Advancements in Biomedical, Optoelectronics, Sensing, and Catalysis Applications. *ACS Applied Bio Materials*. **7**(4), 2086–2127.

[5]. J. Mondal, R. Lamba, Y. Yukta, R. Yadav, R. Kumar, B. Pani, B. Singh, (2024). Advancements in semiconductor quantum dots: expanding frontiers in optoelectronics, analytical sensing, biomedicine, and catalysis. *Journal of Materials Chemistry C*. **12**(28), 10330–10389.

[6]. N. A. Pechnikova, K. Domvri, K. Porpodis, M. S. Istomina, A. V. Iaremenko, A. V. Yaremenko, (2025). Carbon Quantum Dots in Biomedical Applications: Advances, Challenges, and Future Prospects. *Aggregate*. **6**(3).

[7]. K. Bazaka, M. V. Jacob, K. Ostrikov, (2016). Sustainable Life Cycles of Natural-Precursor-Derived Nanocarbons. *Chemical Reviews*. **116**(1), 163–214.

[8]. B. Zhang, Y. Jiang, R. Balasubramanian, (2021). Synthesis, formation mechanisms and applications of biomass-derived carbonaceous materials: A critical review. *Journal of Materials Chemistry A*. **9**(44), 24759–24802.

[9]. M. H. Nguyen, D. T. Le, H. T. Do, A. T. Le, (2024). Remarkable luminescent carbon quantum dots: green synthesis from orange juice using microplasma-liquid method. *Fullerenes Nanotubes and Carbon Nanostructures*. **32**(3), 282–287.

[10]. K. Kasirajan, M. Karunakaran, H. K. Choi, (2024). Synthesis of environmentally-friendly carbon quantum dots from orange juice for selective detection of Fe3+ ions, antibacterial activity, and bio-imaging applications. *Journal of Environmental Chemical Engineering*. **12**(5).

[11]. K. Khurana, N. Jaggi, (2021). Localized Surface Plasmonic Properties of Au and Ag Nanoparticles for Sensors: a Review. *Plasmonics*. **16**(4), 981–999.

[12]. R. K. Sajwan, P. R. Solanki, (2023). Gold@Carbon Quantum Dots Nanocomposites Based Two-In-One Sensor: A Novel Approach for Sensitive Detection of Aminoglycosides Antibiotics in Food Samples. *Food Chemistry*. **415**.

[13]. M. A. Zafar, M. V. Jacob, (2022). Plasma-based synthesis of graphene and applications: a focused review. *Reviews of Modern Plasma Physics*. **6**(1).

[14]. T. Habib, J. M. A. Caiut, B. Caillier, (2024). Fast synthesis of gold nanoparticles by cold atmospheric pressure plasma jet in the presence of Au+ ions and a capping agent. *Plasma Science and Technology*. **26**(7).

[15]. C. Chokradjaroen, X. Wang, J. Niu, T. Fan, N. Saito, (2022). Fundamentals of solution plasma for advanced materials synthesis. *Materials Today Advances*. **14**.

[16]. S. E. Kim, J. C. Yoon, A. Muthurasu, H. Y. Kim, (2024). Functionalized Triangular Carbon Quantum Dot Stabilized Gold Nanoparticles Decorated Boron Nitride Nanosheets Interfaced for Electrochemical Detection of Cardiac Troponin T. *Langmuir*. **40**(47), 25051–25060.

[17]. Q. Zhang, W. Ge, Y. Wang, D. Han, M. Yang, X. Xie, P. He, H. Yin, (2024). A near-infrared fluorescence enhancement strategy of amorphous silicon nanoparticles for night vision imaging and visualizing latent fingerprints. *Journal of Materials Chemistry C*. **12**(33), 12928–12940.

[18]. V. Can, B. Onat, E. S. Cirit, F. Sahin, Z. C. Canbek Ozdil, (2023). Metal-Enhanced Fluorescent Carbon Quantum Dots via One-Pot Solid State Synthesis for Cell Imaging. *ACS Applied Bio Materials*. **6**(5), 1798–1805.

[19]. L. Duan, X. Du, H. Zhao, Y. Sun, W. Liu, (2020). Sensitive and selective sensing system of metallothioneins based on carbon quantum dots and gold nanoparticles. *Analytica Chimica Acta*. **1125**, 177–186.

[20]. S. Ngernpimai, T. Puangmali, A. Kopwitthaya, P. Tippayawat, A. Chompoosor, S. Teerasong, (2024). Enhanced Stability of Gold Nanoparticles with Thioalkylated Carboxyl-Terminated Ligands for Applications in Biosensing. *ACS Applied Nano Materials*. **7**(11), 13124–13133.

[21]. Z. Lu, L. W. Giles, B. M. Teo, R. F. Tabor, (2022). Carbon dots as a 'green' reagent to produce shape and size controlled gold nanoparticles for application in pollutant degradation. *Colloids and Interface Science Communications*. **46**.

[22]. R. K. Sajwan, G. B. V. S. Lakshmi, P. R. Solanki, (2021). Fluorescence tuning behavior of carbon quantum dots with gold nanoparticles via novel intercalation effect of aldicarb. *Food Chemistry*. **340**.

[23]. L. Wang, X. Wang, H. Zhao, (2025). Highly Efficient Luminescent Solar Concentrators Based on Capped Carbon Quantum Dots with Unity Quantum Yield. *Advanced Functional Materials*. **35**(24).

PHÁT QUANG CỦA CHẤM LƯỢNG TỬ CARBON SINH HỌC BIẾN TÍNH VỚI HẠT NANO VÀNG

Lê Anh Thi[1,2], Võ Thanh Tùng[3] , Lâm Thị Bích Trân[4], Đỗ Hoàng Tùng[5], Nguyễn Như Lê[6], Lê Thị Kim Dung[7], Trần Duy Quỳnh Như[7], Nguyễn Minh Hoa[7]*

[1]Viện nghiên cứu và Phát triển, Đại học Duy Tân, Đà Nẵng

[2]Khoa Khoa học tự nhiên, Đại học Duy Tân, Đà Nẵng

[3]Trường Đại học Khoa học, Đại học Huế

[4]Trường Đại học Sư phạm Thành phố Hồ Chí Minh, Gia Lai

[5]Viện Vật lý, Viện Hàn lâm Khoa học và Công nghệ Việt Nam

[6]Khoa Vật lý, Trường Đại học Sư phạm, Đại học Huế

[7]Khoa Khoa học cơ bản, Trường Đại học Y Dược, Đại học Huế

TÓM TẮT

Nghiên cứu này khảo sát quá trình tổng hợp và đặc trưng của chấm lượng tử carbon (CQDs) từ nước cam bằng phương pháp plasma–dung dịch, sau đó chức năng hóa với hạt nano vàng (AuNPs). CQDs cho phát quang xanh mạnh khi kích thích tại 390 nm, với hiệu suất lượng tử đạt 21,9%. CQDs có dạng cầu với kích thước trung bình ~3,5 nm, trong khi AuNPs có kích thước trung bình 18 nm. Các nanohybrid Au@CQDs (NHs) thu được có kích thước tăng lên >20,2 nm. Phổ hấp thụ UV-Vis và huỳnh quang chứng minh sự tương tác giữa CQDs và AuNPs, với các nanohybrid thể hiện sự tăng cường huỳnh quang nhờ hiệu ứng plasmon. Nghiên cứu này đề xuất một phương pháp tổng hợp CQDs thân thiện với môi trường và lai hóa với AuNPs, nhấn mạnh vai trò của biến tính bề mặt đối với đặc tính quang, hứa hẹn ứng dụng trong cảm biến và thiết bị quang tử.

Từ khóa. Chấm lượng tử carbon, phát quang, phytocapped, AuNPs, biến tính bề mặt.

Lê Anh Thi sinh ngày 17/03/1983 tại Gia Lai. Ông tốt nghiệp cử nhân sư phạm Vật lý năm 2007 tại trường Đại học Quy Nhơn, tốt nghiệp Thạc sĩ chuyên ngành Vật lý chất rắn năm 2011 tại Trường Đại học Khoa học, Đại học Huế, Tốt nghiệp Tiến sĩ chuyên ngành Khoa học Vật liệu năm 2025 tại Viện Khoa học vật liệu, Viện HL KH&CN Việt Nam. Ông công tác tại Viện NCPT CNC, Đại học Duy Tân, Đà Nẵng.

Lĩnh vực nghiên cứu: Vật liệu nano, vật lý plasma, khoa học vật liệu.

Võ Thanh Tùng sinh năm 1979 tại Thừa Thiên Huế. Ông tốt nghiệp cử nhân ngành Vật lý học năm 2001 và thạc sĩ ngành Vật lý học năm 2007 tại Trường Đại học Khoa học, ĐHH Huế; nhận học vị tiến sĩ năm 2009 tại Trường Đại học Tổng hợp Quốc gia Belarus. Ông công tác tại Trường Đại học Khoa học, ĐH Huế từ năm 2001.

Lĩnh vực nghiên cứu: Gốm áp điện, Vật lý chất rắn, Mô phỏng vật liệu.

Lâm Thị Bích Trân sinh ngày 11/12/1985 tại Bình Định. Bà tốt nghiệp cử nhân ngành Vật lí tại trường Đại học Qui Nhơn năm 2007, tốt nghiệp thạc sĩ chuyên ngành Lí luận và phương pháp dạy học bộ môn Vật lí năm 2013 tại trường Đại học Sư phạm TP.HCM. Bà công tác tại Trường Đại học Sư phạm TP.HCM – Phân hiệu Gia Lai.

Lĩnh vực nghiên cứu: Vật liệu nano, Vật lý lý thuyết.

Đỗ Hoàng Tùng sinh ngày 27/1/1979 tại Thanh Hoá. Ông tốt nghiệp cử nhân ngành Vật lý lý thuyết tại trường Đại học Khoa học Tự nhiên, Đại học Quốc gia Hà Nội năm 2001, tốt nghiệp Tiến sĩ chuyên ngành Vật lý thực nghiệm năm 2009 tại trường Trường Đại học Greifswald, CHLB Đức. Ông công tác tại Vật lý kỹ thuật; Viện Vật lý; Bộ Viện Hàn lâm Khoa học và Công nghệ Việt Nam.

Lĩnh vực nghiên cứu: Vật lý plasma ứng dụng trong y sinh và nông nghiệp; Vật lý plasma ứng dụng trong khoa học vật liệu và môi trường

Nguyễn Như Lê sinh ngày 22/9/1984 tại Thanh Hoá. Bà tốt nghiệp Cử nhân Sư phạm Vật lý (2006), Thạc sĩ Vật lý lý thuyết và Vật lý toán (2009), và Tiến sĩ Vật lý lý thuyết và Vật lý toán (2017) tại Trường Đại học Sư phạm, Đại học Huế. Từ năm 2008 đến nay, Bà là giảng viên Khoa Vật lý, Trường Đại học Sư phạm, Đại học Huế.

Lĩnh vực nghiên cứu: phản ứng thiên văn hạt nhân, phản ứng tán xạ hạt nhân trong mô hình vi mô, quá trình tổng hợp và phân rã hạt nhân nặng và siêu nặng.

Lê Thị Kim Dung sinh ngày 08/11/1984 tại Thành phố Huế. Năm 2022, bà tốt nghiệp tiến sĩ chuyên ngành Hóa Phân tích tại Trường Đại học Khoa học, Đại học Huế. Bà công tác tại trường Đại học Y Dược, Đại học Huế từ năm 2009 đến nay.

Lĩnh vực nghiên cứu: Hóa phân tích, Điện hóa.

Trần Duy Quỳnh Như sinh ngày 15/09/1997 tại Thành phố Huế. Bà tốt nghiệp cử nhân chuyên ngành Vật lí tại trường Đại học Sư phạm, ĐH Huế năm 2019. Bà công tác tại trường Đại học Y Dược, ĐH Huế từ năm 2019 đến nay.

Lĩnh vực nghiên cứu: Khoa học vật liệu

Nguyễn Minh Hoa sinh ngày 28/6/1985 tại Hà Tĩnh. Bà tốt nghiệp Cử nhân Sư phạm Vật lý (2007) và Thạc sĩ Lý luận và phương pháp dạy học Vật lý (2012) tại Trường Đại học Sư phạm, Đại học Huế, và Tiến sĩ Vật lý lý thuyết và Toán lý (2020) tại Trường Đại học Sư phạm Hà Nội. Bà công tác tại Trường Đại học Y Dược, Đại học Huế từ năm 2012, hiện là giảng viên chính Bộ môn Hóa học – Lý sinh, Khoa Cơ bản.

Lĩnh vực nghiên cứu: Vật lý lý thuyết, Vật liệu nano, Vật lý plasma ứng dụng trong y sinh và khoa học vật liệu.